Emission of photons in spontaneous fission of ^{252}Cf

H. van der Ploeg, J. C. S. Bacelar, A. Buda, C. R. Laurens, and A. van der Woude
Kernfysisch Versneller Instituut, 9747 AA Groningen, The Netherlands

J. J. Gaardhøje and Z. Żelazny
Niels Bohr Instituut, Tandem Accelerator Laboratory, Risø, Denmark

G. van 't Hof and N. Kalantar-Nayestanaki*
Faculteit der natuurkunde en sterrenkunde, Vrije Universiteit, De Boelelaan 1081, 1081 HV, Amsterdam, The Netherlands

(Received 23 January 1995)

High energy photon emission accompanying the spontaneous fission of ^{252}Cf is measured for different mass splits. The photon yields up to an energy of 20 MeV are obtained at several angles relative to the fission direction. Statistical model calculations are used to interpret the data. The photon yield is found to be very sensitive to the initial excitation energy sharing among the daughter nuclei and to their level density parameters. Using experimentally extracted level densities obtained from neutron evaporation measurements, the photon yield is well described by calculations for all mass splits.

PACS number(s): 25.85.Ca, 24.30.Cz, 27.90.+b, 21.10.Ma

I. INTRODUCTION

The dynamics of the fission process [1] has recently become an important topic of research. This revival followed the observation that the multiplicity of emitted prescission neutrons [2,3] and γ rays [4] was much larger than expected. This observation implies in a rather model-independent way that the fission process has a time delay which is longer than expected from statistical considerations. Several experiments using fusion-fission reactions were used to quantify these observations [2–6]. The difficulty with these studies is that the fission fragments produced in fusion-fission reactions emit themselves significant numbers of "postscission" neutrons and γ rays. In order to analyze the prescission yields, the postscission contribution has to be accurately estimated.

Neutron angular distributions with respect to the fission direction provide a possible method to separate the postscission and prescission neutron contributions [2,3]. The prescission γ-ray multiplicity, which is also a sensitive fission time clock [4], requires the subtraction of the postscission contribution from the total γ-ray spectrum. This can only be done by a statistical model calculation of the postscission contribution. In order to check these calculations and to determine the relevant parameters values, one can compare them to experimental data for the spontaneous fission of ^{252}Cf [7]. Up to the present study the only data available for the mass-dependent γ-ray yields obtained for ^{252}Cf extended up to γ-ray energies of 6–8 MeV [8]. Measurements without mass identification were also reported by other groups [9–13]. However, the extract the fission time delay, the in-beam studies require precise knowledge of the γ-ray yield in the giant resonance region, i.e., in the photon energy range of 10–20 MeV.

In the present work we report on a high statistics experiment performed to measure the γ-ray yield up to 20 MeV associated with the spontaneous fission of ^{252}Cf. The results of an earlier experiment have already been published [12]. The experimental measured yield of photons with energies $E_\gamma > 20$ MeV is discussed elsewhere [14]. The measured γ-ray yield as a function of the mass split between the two fission fragments is found to be highly sensitive to the initial excitation energy sharing among the two fragments and to their level densities parameters. Using experimentally extracted level densities and initial excitation energies obtained from neutron evaporation measurements accompanying the spontaneous fission of ^{252}Cf [15], the photon yields are well described by calculations for all mass splits. In addition we have measured the γ-ray angular distribution with respect to the fission direction for postscission photons, in order to investigate the previously reported anomalous result [12,13].

The methods and assumptions used in the present analysis are described in Sec. II and the predicted postscission γ-ray yields from the spontaneous fission decay of ^{252}Cf are shown. In Sec. III, the experimental arrangement is described. The mass dependence of the γ-ray yields is discussed in Sec. IV, and the angular correlation with respect to the fission direction in Sec. V. Conclusions derived from this work are summarized in Sec. VI.

II. POSTSCISSION γ-RAY EMISSION PROBABILITIES FOR ^{252}Cf

In order to calculate the γ-ray and neuron emission probabilities accompanying the spontaneous fission of ^{252}Cf, a modified version of the statistical code CASCADE [16] was used. This code calculates the statistical decay rates using the Hauser-Feshbach formalism, starting from a matrix representing the initial population probability of excited states of each fission fragment with a given A and Z. The high energy photon emission probability was calculated using a double

*Current address: Kernfysisch Versneller Instituut, 9747 AA Groningen, The Netherlands.

Lorentzian curve for the giant dipole resonance (GDR) strength function [17,18], with a given width and centroid energy. The GDR width is parametrized as [20] $\Gamma_{\mathrm{GDR}}=4.8+0.0026E_{\mathrm{exc}}^{1.6}$ MeV, which is consistent with experimental data [18–20] for nuclei in the mass region $100<A<160$. The GDR centroid energy was parametrized as $E_{\mathrm{GDR}}=31.2A^{-1/3}+20.6A^{-1/6}$ MeV from the systematics [21] of GDR studies on the ground sate of nuclei. This relation is very similar, within the nuclear mass range considered in the present studies, to the proposed parametrization of the GDR centroid energy built on highly excited states [18]. The splitting of the strength distribution was calculated for an average prolate deformation of $\beta=0.24$ [22], but the final results are not sensitive to this energy splitting. The width of the two components is given by the relation $\Gamma_i=\Gamma_{\beta=0}(E_i/E_{\beta=0})^2$ [23–25].

The probability $\mathcal{P}(A_1,Z_1,E_1^{\mathrm{exc}},I_1,A_2,Z_2,E_2^{\mathrm{exc}},I_2)$ of populating a given pair of daughter nuclei with particular values of excitation energy E^{exc} (collective and noncollective) and angular momentum (I) can be calculated analytically [12,7]. For this purpose [see Eq. (1) below], the experimentally determined mass distribution as well as the mean and variance of the kinetic energy (E^{kin}) measured as a function of fragment mass have been used [15,26].

The total excitation energy (E^{exc}) available for both fragments follows from the energy balance:

$$E^{\mathrm{exc}}(A_1,A_2)=Q(A_1,A_2)-E^{\mathrm{kin}}(A_1,A_2). \tag{1}$$

Here $Q(A_1,A_2)$ is the Q value for a particular mass split. Three different contributions to the total excitation energy are considered, namely, deformation energy (E^{def}), noncollective excitation energy, and rotational energy (E^{rot}). The deformation energy is determined by using the calculation deformation parameters at the scission point taken from Ref. [27] and the corresponding deformation potentials from the liquid drop model for slightly deformed spheres [28]. The noncollective excitation energy or thermal energy is divided among the fission fragments assuming a uniform temperature at the scission point. The rotational energy is calculated using the measured [29] average fragment angular momentum of $J=6\hbar$ with a full width at half maximum (FWHM) of $2\hbar$ and with a moment of inertia obtained from the calculated deformation parameters at scission [27]. Shortly after scission the deformation energy stored by each fragment is converted into internal excitation energy. It is assumed that the time scale for shape equilibration is fast and the statistical decay process starts from completely equilibrated states of both fragments. Therefore the excitation energy for a particular fission fragment is given by

$$E_1^{\mathrm{exc}}=E_1^{\mathrm{def}}+\frac{A_1}{A_1+A_2}(Q_{1,2}-E_1^{\mathrm{kin}}-E_2^{\mathrm{kin}}-E_1^{\mathrm{def}} -E_2^{\mathrm{def}}-E_1^{\mathrm{rot}}-E_2^{\mathrm{rot}}). \tag{2}$$

The excitation energy of the complementary fragment with mass A_2 is calculated analogously. An assumption has to be made on how the experimental, mass-dependent, variance in the kinetic energy is distributed. Here, it is assumed that the variance in the total excitation energy (which is equal to the variance in the kinetic energy) is redistributed

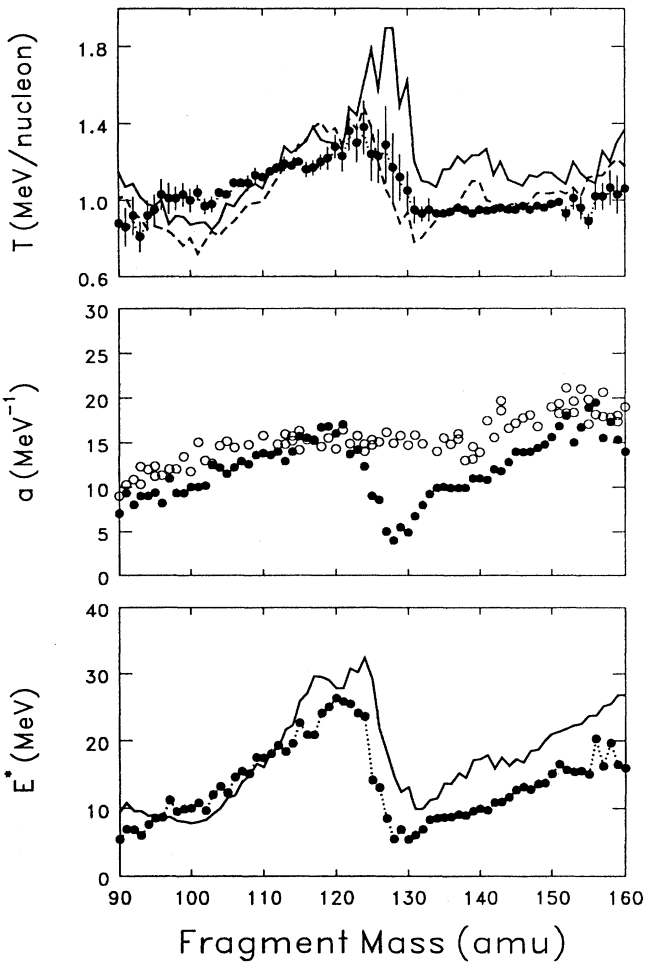

FIG. 1. Experimentally determined [15] temperature (T), level density parameters $a(E^*=aT^2)$, and excitation energy E^*, for fragments accompanying the spontaneous fission of ^{252}Cf (full dots). The open dots represent the Dilg *et al.* [30] level density parameters. The curves drawn are obtained from different assumptions used to determine the excitation energy and temperature of the initial populated state in the fission fragments.

over the two fission fragments in such a way that it scales directly with the fragment excitation energy [7]:

$$\sigma^2_{E_1^{\mathrm{exc}}}=\frac{E_1^{\mathrm{exc}}}{E_1^{\mathrm{exc}}+E_2^{\mathrm{exc}}}\,\sigma^2_{E_{\mathrm{kin}}}. \tag{3}$$

The model, described above to calculate excitation energies for the fragments of the spontaneous fissioning ^{252}Cf nuclei, can be compared with recent measurings [15] performed with a ^{252}Cf source (see Fig. 1). In that quite extensive work the excitation energy was evaluated from measured mean neutron multiplicities ($\bar{\nu}$), average neutron kinetic energy ($\bar{\eta}$), and average γ-ray energy ($\bar{E}_\gamma$). These measurements are then combined with the neutron binding energy (B_n) in order to extract an experimental value of the total excitation energy available for a specific mass split and kinetic energy $[E^{\mathrm{exc}}(A_1,E_{\mathrm{kin}}),E^{\mathrm{exc}}(A_2,E_{\mathrm{kin}})]$:

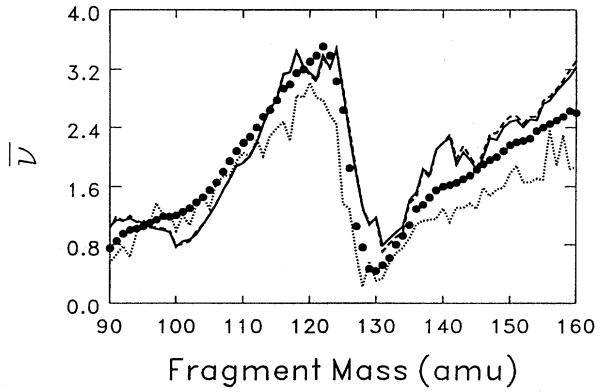

FIG. 2. Measured neutron multiplicities ($\bar{\nu}_n$) accompanying the spontaneous fission of ^{252}Cf (full dots). The curves drawn are the results of three CASCADE calculations: the solid curve uses calculated excitation energies [Eqs. (2) and (3)] and level density parameters from [15]; the dashed curve uses instead the Dilg *et al.* [30] level density parameters; the dotted curve uses for both the excitation energy and level density parameters the experimentally determined values from Ref. [15].

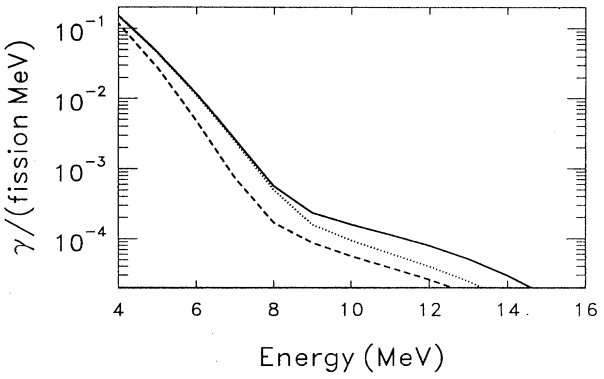

FIG. 3. Calculated γ-ray emission probabilities for the spontaneous fission of ^{252}Cf. The different CASCADE input parameters are described in the text and the caption of Fig. 2.

$$E^{\mathrm{exc}}(A,E_{\mathrm{kin}})=\bar{\nu}(A,E_{\mathrm{kin}})[B_n(A,Z)+\bar{\eta}(A,E_{\mathrm{kin}})] + \bar{E}_{\gamma}(A,E_{\mathrm{kin}}). \quad (4)$$

The nuclear temperatures as a function of the fragment mass and kinetic energy as also experimentally deduced in Ref. [15] from the energy spectra of neutrons emitted in the center-of-mass reference system. The effective, mass-dependent level density parameters a were deduced from the slope between the square of the temperatures, $T^2(A,E_{\mathrm{kin}})$, and the estimated nuclear excitation energies $E_{\mathrm{exc}}(A,E_{\mathrm{kin}})$: $E_{\mathrm{exc}}=aT^2$. The kinetic energy averaged temperatures and excitations energies are shown in Fig. 1.

Our CASCADE predictions for the postscission neutron multiplicities are compared with the measured neutron multiplicities in Fig. 2. Since the neutron multiplicity is closely connected to the γ-ray yields for $E_{\gamma}\geq 6$ MeV, the reproduction of the well known zigzag behavior of the neutron multiplicity by CASCADE calculations is of great importance. The solid curve uses the analytical model described above to calculate the excitation energy in the fragments [Eqs. (2) and (3)], and the experimentally determined level density parameters for ^{252}Cf from Ref. [15]. The dashed curve uses level density parameters taken from Dilg *et al.* [30]. (Note that these level density parameters are often used to calculate the postscission γ-ray energy spectra of in-beam studies.) The difference in the level density parameters is shown in Fig. 1. A third CASCADE calculation is shown (dotted curve) in which both the experimentally determined [15] initial excitation energies and level density parameters are used. Therefore the dotted curve goes through the measured data points for both the initial excitation energy and temperatures (see Fig. 1).

As can be seen in Fig. 2 the experimental mass-dependent neutron multiplicity is equally well reproduced by all three calculations on an absolute scale, in spite of the fact that the initial temperatures and excitation energy of the fragments are different for the different models.

Using these three different ways to describe the initial excitation energy and temperatures (level densities) for different mass splits, predictions for the γ-ray multiplicity per fission are shown in Fig. 3. As can be seen in this figure the dashed curve is very different form the other two. This is a result of the different level densities used, which differ in particular for the heavy fragment of a specific mass split (see Fig. 1). The difference between solid and dotted curves originates from the different excitation energies used (see Fig. 1). The larger excitation energies (solid curve) give a larger γ-ray multiplicity for photons emitted above the neutron binding energy (i.e., $E_{\gamma}\geq 8$ MeV). For the more realistic calculations, using experimentally determined [15] level density parameters and initial excitation energies for the fragments populated in the spontaneous fission process of ^{252}Cf, the predictions of the CASCADE calculations are shown in Fig. 4 for different mass splits. Here a strong dependence of the γ-ray yields, especially in the energy region $E_{\gamma}>4$ MeV, is clearly seen.

III. EXPERIMENTAL SETUP

In order to measure the γ rays in the energy range $3<E_{\gamma}<70$ MeV coming from the spontaneous fission of ^{252}Cf, ten large volume (2.6 liter) BaF_2 crystals and a $\varnothing 25.5\times 35.5$ cm^3 NaI [31] crystal were used. The cylindrical crystal of the NaI spectrometer is surrounded by a plastic anticoincidence shield and a lead shield. The NaI spectrometer with a lead collimator of 160 mm diameter was placed at a distance of 795 mm, covering a solid angle of 32 msr. Eight of the ten BaF_2 detectors used are part of the HECTOR array [32]. These detectors are equipped with a temperature stabilized light emitting diode (LED), in order to continuously check the gain stability. Every tenth of a second the LED induced an event in which light of a particular wavelength was directed on the crystal. Seven BaF_2 detectors were placed at a distance of 280 mm from the source, each covering an angle of about 144 msr (see Fig. 5).

Four position-sensitive parallel plate avalanche counters (PPAC's) were used to detect both fission fragments in coincidence, thus allowing the determination of their masses. The PPAC's were positioned in such a way as to cover two an-

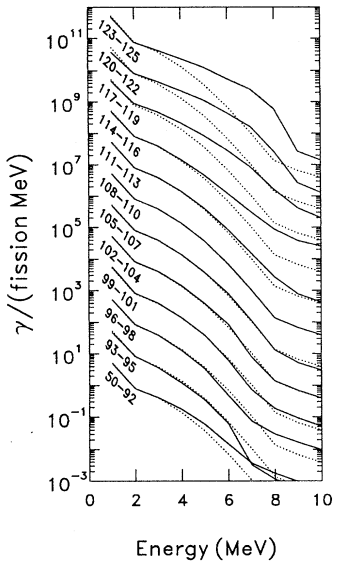

FIG. 4. Calculated γ-ray emission probabilities for the spontaneous fission of ^{252}Cf, as a function of the mass split (full curve). Each mass range is compared with a reference spectrum, being that calculated for the mass split 108–110 and 142–144 amu (dotted curve).

gular regions centered around orthogonal fission directions. High energy photons emitted during the fission process could be detected either along, perpendicular, or at an angle of 45° to the direction defined by the PPAC's (see Fig. 5). PPAC's 1 and 2 (with an active area of 290×190 mm^2) were placed at a distance of 132.5 mm. PPAC's 3 and 4 (180 ×182 mm^2) were placed at a distance of 106 and 119 mm, respectively. When coincidences between two opposite PPAC's are considered, the solid angles for the first (1 and 2) and the second pair (3 and 4) are 2.2 and 1.9 sr, respectively. The PPAC's allow for the determination of position and time of a particle entering the detector.

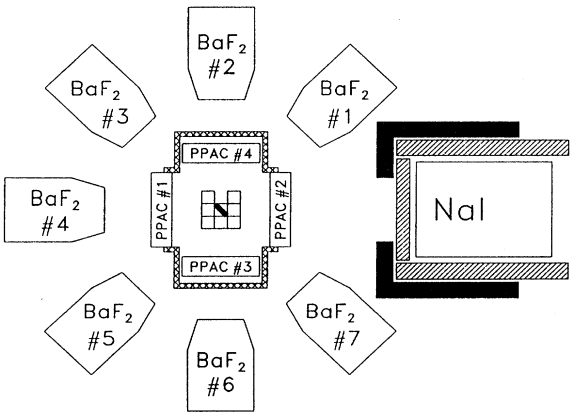

FIG. 5. Experimental setup. The ^{252}Cf source is placed in the middle and in such a way that it faces both pairs of PPAC's. The NaI spectrometer is surrounded by a plastic shield (hatched) and lead shield (black). The eight squares depicted in the middle represent the array of small volume BaF_2 detectors, which are placed out of plane.

An array of eight small volume (35×35×60 mm^3) BaF_2 detectors was placed as close as possible to the source position in order to determine the starting time of each event. With a distance between source and the BaF_2 array of 40 mm, these detectors covered a solid angle of about 2.7 sr. The energy thresholds were set at about 200 keV, just above the noise level. With their good time resolution of less than 1 ns and their high γ-ray efficiency, the array of small volume BaF_2 detectors provide a trigger for the determination of the starting time of each event. The precise determination of the relative time of flight measured by the large volume BaF_2 detectors and NaI spectrometer makes it possible to distinguish prompt γ rays from neutrons (also detected with significant efficiency by the large volume crystals). The times of flight of two opposing PPAC's allow for the determination of both fragment masses.

All seven large volume BaF_2 detectors, the NaI spectrometer, and the PPAC's shown in Fig. 5 are located in one plane. Two large volume BaF_2 detectors (not shown) and the small volume BaF_2 array were placed perpendicular to the plane defined by the PPAC's and the eight large volume crystals. Another large volume BaF_2 detector (not shown in Fig. 5) was placed as far as possible from the source position, but within the experimental room. This detector was used to measure the cosmic-ray energy background spectrum within the experimental room.

A number of different event types were collected during the experiment. The main event type consisted of a fourfold coincidence between a signal from the small BaF_2 detector array, a signal from one of the large volume crystals, and both fission fragments detected in two opposite PPAC's. A second event type was defined by the LED pulser, which was used to check the gain stability of the large volume BaF_2 detectors. A third event type consisted of single events detected by the extra BaF_2 detector, which was used to measure the cosmic-ray background energy spectrum. Scaled-down single events were also recorded on tape for all detector types. The simultaneous collection of different single and coincident event types allows for the determination of the efficiency of each detector system separately.

The activity of the used ^{252}Cf source was 7 μCi. The source was produced by electrodeposition of diffusion bonded Cf_2O_3 on a 1.1 μm thick Ni (and 30 nm Au) backing. The cover was identical to the backing. The active diameter was 3 mm. The total data taking took place over a period of six months in a temperature stabilized experimental room.

All large volume BaF_2 detectors have been calibrated during the experiment using the 4.44 and the 6.13 MeV γ rays coming from a mixed ^{241}Am-^{9}Be source and a mixed ^{244}Cm-^{13}C source, respectively. Previous experiments have determined the response function of these detectors up to 21 MeV [32,14].

The mass of the fission fragments is determined as follows. For each pair of fission fragment masses, the average kinetic energy ($E_{\rm kin}$) is taken from Ref. [26]. The charge of the fission fragments is taken such that its charge-to-mass ratio equals that of ^{252}Cf. From the position information sup-

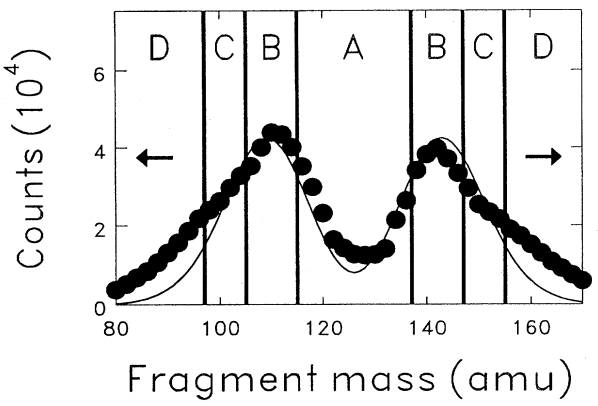

FIG. 6. The experimental fragment mass distribution (full dots). The vertical thick solid lines indicate the boundaries of the four different mass gates. The curve shows the expected mass distribution.

plied by the PPAC's, the amount of Ni-traversed is determined and the energy loss of the fragments is calculated: $E_{\rm loss}(E_{\rm kin},A,Z,d_{\rm Ni})$. This yields the kinetic energies $(E_{\rm kin}-E_{\rm loss})$ after traversing the Ni foil for a particular mass split. There is a one to one correspondence between the calculated velocities and the initial masses for each angle of emission. The velocity of the fission fragments is determined from both time and position information supplied by the PPAC's. The obtained theoretical times of flight are allowed to deviate from the measured times of flight such that the deviation is within the width [27] of the kinetic energies and the PPAC's time resolution, without violating momentum and mass conservation. If the last two conditions cannot be satisfied, the event is rejected. The FWHM in the mass determination is about 10 amu. The experimental mass distribution is shown in Fig. 6. The solid curve in this figure represents a very precise measurement of the fragment mass distribution from Ref. [26], folded with a Gaussian width of 10 amu. Our measurements are in overall agreement with those of Ref. [26], apart from a noticeable deviation for the largest mass splits. This deviation might be caused by the particularly large amount of energy loss associated with these extreme mass splits, whilst moving through the Ni cover of the Cf source. Also angle straggling of the fission fragments in the Ni cover might be a cause for the observed deviation.

IV. MASS DEPENDENCE OF THE γ-RAY EMISSION PROBABILITY

In order to investigate the mass dependence of the γ-ray emission probability, four mass gates were selected (shown in Fig. 6). Furthermore, the data discussed in this section are restricted to the γ-ray yields at $90°\pm35°$ with respect to the fission direction. At other angles the influence of neutron induced pileup effects is significant (see below) and the procedure used to correct for this effect in the photon spectra might introduce systematic errors.

The measured γ-ray emission probabilities in the angular region around 90° with respect to the fission direction are shown in Fig. 7. These spectra are gated by the prompt (photon) peak in the time-of-flight spectrum, whereby random coincidences and cosmic-ray contributions have been subtracted. The mass gates are (see also Fig. 6) symmetric fis-

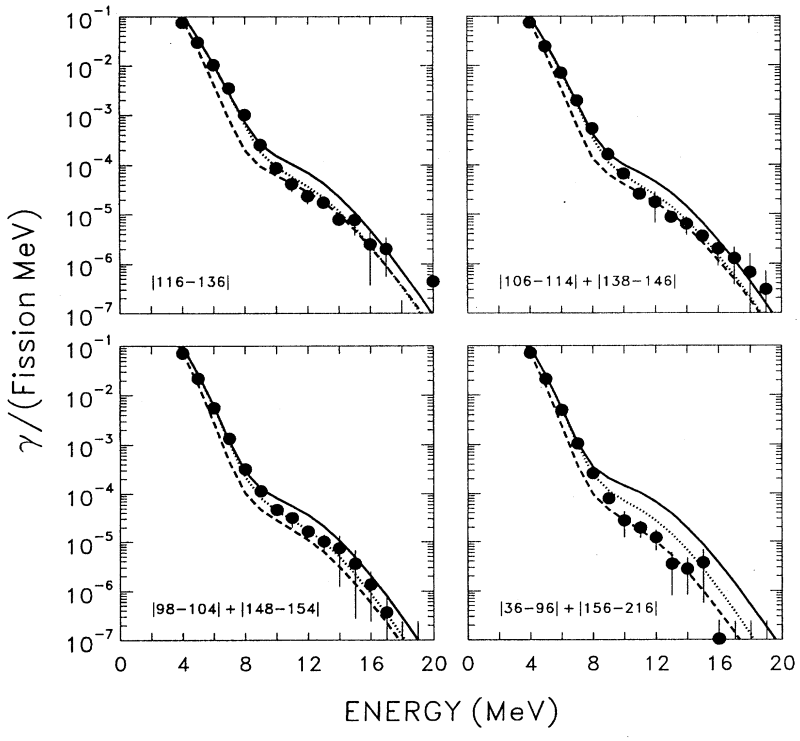

FIG. 7. The photon emission probability at 90° with respect to the fission direction for different mass regions, between fission fragment masses m_1 and m_2, labeled by $|m_1-m_2|$. The error bars indicate statistical and systematic errors. The curves drawn are mass gated CASCADE calculations which are described in the text and in the caption of Fig. 2.

sion with masses between 116 and 136 amu; asymmetric mass splits around the peak of the mass distribution with masses between 106–114 and 138–146 amu; the tail of the mass distribution with masses between 98–104 and 148–154 amu; and the remaining masses between 36–96 and 156–216 amu. All mass gates include both light and heavy fragments, since the detected γ ray cannot be assigned to a specific fission fragment. The curves drawn are CASCADE calculations of the γ-ray emission probabilities (see Sec. II) and corresponds to the conventions used in Figs. 1–3. They are the sum of γ-ray spectra, calculated individually for all possible fission fragment masses and weighted according to the relevant mass distribution. It should be noted that, sine the data are given as the γ-ray yield per fission fragment, the data and the calculations are shown on an absolute scale.

As shown in Fig. 7 the CASCADE calculations using both the excitation energies and level density parameters inferred from the neutron measurements (dotted curve) give quite a good fit to our measured γ-ray yields for all but the most extreme mass gates. When using the model in which the initial excitation energy of each fragment is estimated from the fission dynamics [Eqs. (2) and (3)], the γ-ray spectra calculated by CASCADE show clear deviations from the data. The combination with the level density parameters of Dilg *et al.* [30] (dashed curve) seems to reproduce the spectra in the GDR region but clearly underpredicts the γ-ray yield in the range $4 \leq E_\gamma \leq 10$ MeV. Using the level density parameters of Budtz-Jørgensen and Knitter [15] inferred for the fission fragments of ^{252}Cf (solid curve) the calculations describe well the low energy photon yields, but strongly overestimate (by about a factor of 2) the γ-ray yields in the giant dipole resonance region ($10 \leq E_\gamma \leq 20$ MeV). The results clearly show the high sensitivity of the fission-coincidence postscission photon spectrum to both the fragment excitation energy and the level density parameter.

The disagreement between the best CASCADE calculations (represented by the dotted curve in Fig. 7) and the data for very asymmetric mass splits might be correlated to the significant difference between the experimental mass distribution and the expected masses distribution for this particular mass gate (see Fig. 6).

In Ref. [8] an enhancement was found in the γ-ray emission probability in the energy region between 2 and 8 MeV for symmetric mass splits when compared with more asymmetric mass splits. The quantitative analysis performed for our data with the help of the CASCADE statistical decay code reproduces the trend in the spectral differences found in the photon energy region 2–8 MeV as a function of the mass split (see Fig. 4). The small level density parameters a for fission fragment masses around $A \approx 132$ (see Fig. 1) give rise to the enhancement of the γ-ray emission probability between and 4 and 8 MeV. These γ-ray emission probabilities are predominantly sensitive to the level density parameters a and almost independent of the initial excitation energy. The a values have been taken from neutron measurements [15] where they are deduced from both initial excitation energy and temperature. The observed mass dependence in the γ-ray emission probability between 4 and 8 MeV can only be reproduced using these mass-dependent a values.

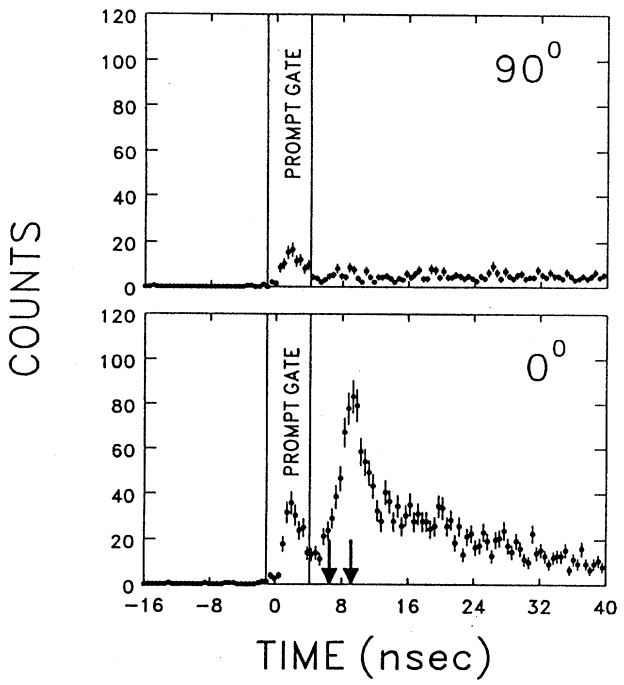

FIG. 8. Time-of-flight spectra for a 1 MeV energy interval centered around 9 MeV energy which is detected in one large volume BaF_2 detector, at 90° and 0° with respect to the fission direction, respectively. The arrows drawn indicate the time of flight for neutrons. The right arrow gives the time for the most probable neutron energy. The left arrow corresponds to the time of flight of those neutrons which are converted into photons in PPAC or chamber material.

V. ANGULAR DEPENDENCE OF THE γ-RAY EMISSION PROBABILITY

Neutrons in the center-of-mass frame of each fission fragment are predominantly emitted isotropically. When transforming the isotropic neutron emission from the center-of-mass system to the laboratory system, the neutrons are highly focused in the direction of the velocity vector of a particular fission fragment. Therefore, in the laboratory, the emitted neutrons have a pronounced angular dependence with respect to the fission direction. From the time-of-flight spectra of the large volume BaF^2 detectors, the relative event rate due to neutrons with respect to the fission direction was measured. As shown in Fig. 8, neutrons emitted from the source do not contribute significantly to the prompt (photon) time-of-flight peak. Even when they would produce a γ ray in the material surrounding the source, in which case part of the distance between source and detector is now traversed at the speed of light, the resulting time of flight decreases to 6.5 nsec, well outside the γ time gate (see left arrow depicted in Fig. 8). A conservative upper limit for neutrons converted into γ rays in the PPAC and chamber material is calculated to be 1×10^{-4} detected γ rays per fission. The only contribution from neutrons to the prompt time-of-flight peak could arise from neutrons which convert into γ rays at the source position. The upper limit for the probability of neutrons in-

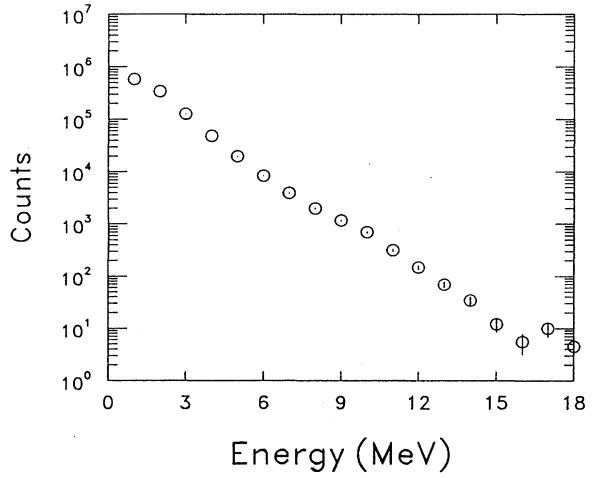

FIG. 9. The neutron spectrum inferred from an analysis of the time-of-flight spectrum at different energy intervals deposited in the BaF_2 detectors used.

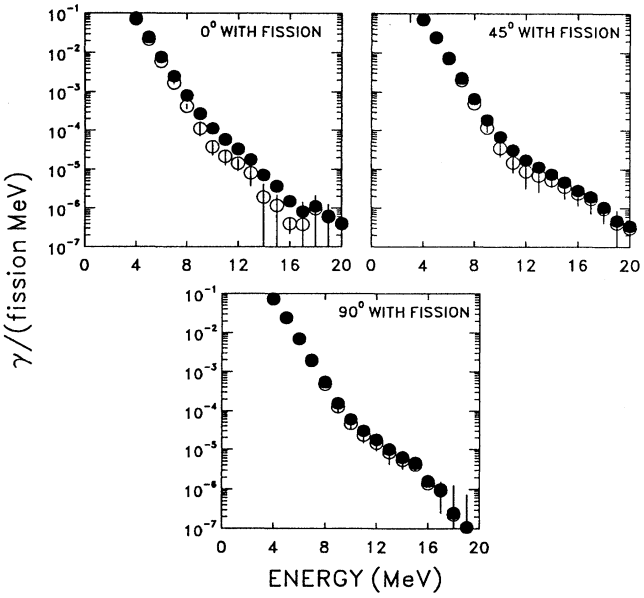

FIG. 10. The photon emission probability at 0°, 45°, and 90° with respect to the fission direction. The closed dots represent the data uncorrected for neutron induced prompt pileup. The open dots represent the corrected data. The error bars are due to the statistical and systematic errors.

teracting in the thin Ni foil which covers the ^{252}Cf source is 3×10^{-9} and this can be neglected.

The ^{252}Cf source used in these studies to investigate the γ-ray emission probabilities has a strength corresponding to 8000 fissions per second. This in combination with the efficiency of the BaF_2 detectors used results in a negligible random pileup rate. However, "prompt pileup" or summing effects, specially those induced by neutrons, significantly contribute to the observed γ-ray spectra at 0° and 45°. The term "prompt pileup" means that particles or γ rays which originate from the same fission event as the initial γ ray that defines the event hit the same BaF_2 detector within the 1 μsec charge integration time used to analyze the original γ ray. Specifically, neutrons enter the large volume BaF_2 detector between 8 and 24 nsec after a γ ray (see Fig. 8) from the same fission event. Therefore, in order to obtain "clean" γ-ray spectra this neutron induced "prompt pileup" contribution has to be calculated and then subtracted. The neutron spectrum (see Fig. 9), as measured by a BaF_2 detector, has been obtained by integrating for each energy bin all the events outside the γ-ray peak (see Fig. 8). The γ-ray spectrum at 90°, which has a minimum neutron contribution (see Fig. 8) is then convoluted with the angle-dependent neutron yields, in order to create the "prompt pileup" spectra.

The calculated angle-dependent neutron induced "prompt pileup" contribution is then subtracted from the measured γ-ray spectra at 0°, 45°, and 90° with respect to the fission direction. The uncorrected and corrected γ-ray emission probabilities are compared to each other in Fig. 10. As expected, the influence of prompt neutron pileup on the measured γ-ray emission probability at 90° with respect to fission is minimal.

The corrected γ-ray spectra for 0° and 90° with respect to fission are divided by each other and the resulting anisotropy $[W(0°)/W(90°]$ is shown in Fig. 11. As is clear from this figure, the large anisotropy obtained from the uncorrected data as presented in Refs. [12,13] (also included in Fig. 11) is caused by prompt pile up events. The curves in Fig. 11 indicate the anisotropy due to Doppler shift effects of the emitted γ rays. Given the method used to correct for the pileup effect and the possibility that there are systemic errors involved, it is not obvious whether the corrected anisotropy at energies around 10 MeV is significant.

For the 0° measurements it is possible to determine which fragment (light or heavy) is moving towards or away from the γ-ray detector under consideration, since the individual mass of each fragment is measured. The resulting data are presented as the ratio of the γ-ray spectrum measured whenever the light fragment is moving towards W(LT) to the γ-ray spectrum measured whenever the light fragment is moving away from W(LA) the γ-ray detector (see Fig. 12). Due to Doppler shift effects one can expect that W(LT) $\neq W$(LA). Whenever the γ-ray emission probability originating from the light fragments dominates that coming from the heavy fragments, Doppler shift effects will cause the above defined ratio to be larger than 1. So this observable is sensitive to the calculated γ-ray yields for each fragment separately. Our data indicate that the assumed initial excitation energy and level density parameters for individual fragments for each mass split are correctly determined. The calculation using the model predicted fragment excitation energies and the Dilg level density parameters (dashed curve) overestimates the observed ratio in the energy range 3–9 MeV, while the other two calculations (solid and dotted curves) reproduce the data equally well. It can be seen from Fig. 12 that the γ-ray emission probability coming from the heavy fragments dominates that coming from the light fragments at energies around 8 MeV.

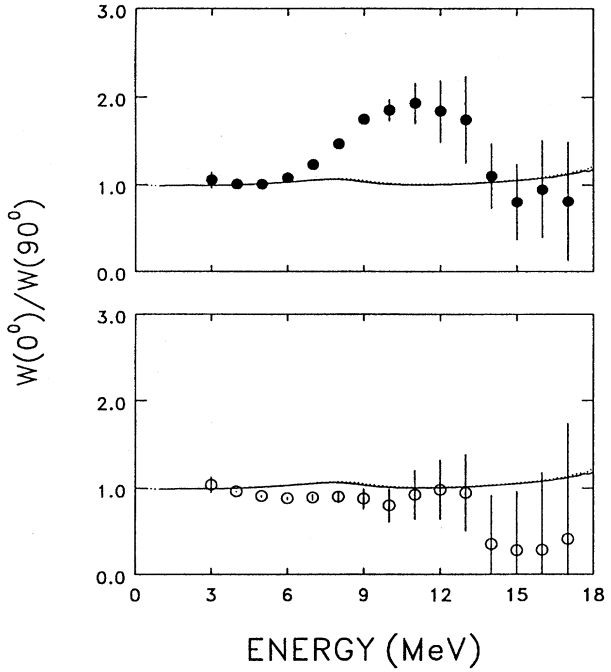

FIG. 11. The measured angular anisotropy $W(0°)/W(90°)$ corrected for neutron induced prompt pileup (open dots) and uncorrected (full dots). The curves drawn show CASCADE calculations described in the text and in the caption of Fig. 2. The calculated anisotropy is due to the Doppler shift effects in the γ-ray emission in the laboratory frame.

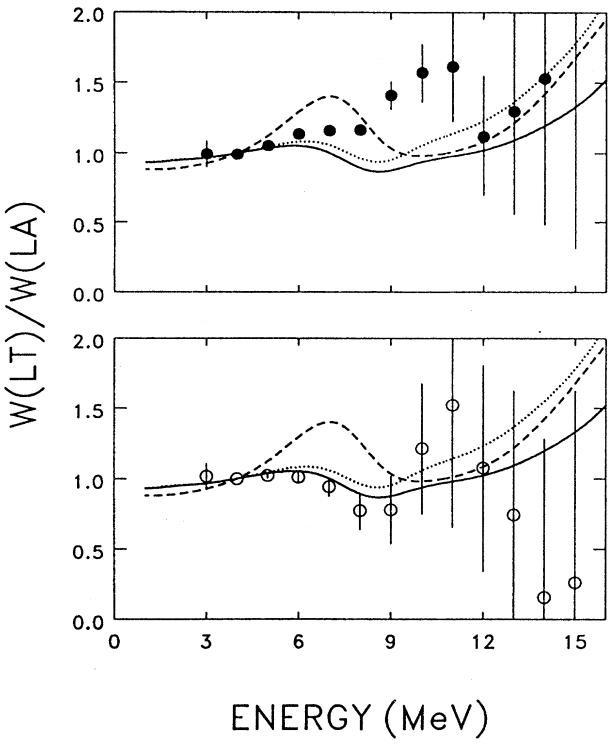

FIG. 12. Division of the γ-ray spectrum measured for light fragments moving towards the γ-ray detector under consideration by the spectrum measured for light fragments moving away from the γ-ray detector. The data points have been corrected for neutron induced pileup effects. The curves drawn show CASCADE calculations including Doppler shift corrections (see text and caption of Fig. 2).

VI. CONCLUSIONS

In summary, for the spontaneous fission of ^{252}Cf the γ-ray emission probability between 3 and 20 MeV has been found to be dependent on the particular mass division between the two fragments. The mass dependence between 4 and 8 MeV is predominantly determined by the level density parameter a, wheel for the remaining part above $E_\gamma > 8$ MeV both a and the initial excitation energy E^* are important. The data can be quite well explained by a statistical model calculation in which both the initial excitation energies and level density parameters are inferred from previous neutron measurements [15]. When using a model describing the fission process to estimate the initial excitation energy of both fragments the γ-ray spectra calculated by CASCADE show clear deviations from the data.

The Doppler shift effects in the 0° (180°) spectra can be reproduced by statistical model calculations using the mass-dependent level density parameters.

Comparing the result of the CASCADE calculations for the neutron multiplicity and the γ-ray emission probability in the GDR region ($E_\gamma > 8$ MeV), we observe that the latter is more sensitive rot the initial excitation energy of the two fission fragments. The mass-dependent level density parameters a used in the present calculations should also be used in the statistical model predictions of the postfission γ-ray contribution of those fusion-fission experiments for which the mass range of the fission fragments and the excitation energies are comparable with that of ^{252}Cf (SF). The latter requirement is fulfilled in fusion-fission processes with long fission time scales, where most of the excitation energy is taken away by prescission neutron emission.

A careful determination of the γ-ray angular distribution shows a small anisotropy in the γ-ray emission probability with respect to the fission direction. However, this may be due to the systematic errors in the correction procedure. It has been found that the large enhancement previously reported [12,13] can be attributed to the large distortion inflicted by neutron induced "prompt pileup" on the measured γ-ray spectra, especially on the one obtained at 0° with respect to fission.

ACKNOWLEDGMENTS

This work has been supported by the stichting Fundamenteel Onderzoek der Materie (FOM) which is financially supported by the Nederlandse Organisatie voor Wetenschapelijk Onderzoek (NWO). J.J.G. and Z.Ż. acknowledge the support of the Danish Science Research Foundation and the Carlsberg Foundation.

[1] *Proceedings of the International Conference on Fifty Years Research in Nuclear Fission* [Nucl. Phys. **A502** (1989)], and references therein.
[2] D. J. Hinde, D. Hilscher, H. Rossner, B. Gebauer, M. Lehmass, and M. Wilpert, Phys. Rev. C **45**, 1229 (1992).
[3] D. Hilscher and H. Rossner, Ann. Phys. (Paris) **17**, 471 (1992), and references therein.
[4] P. Paul and M. Thoennessen, Annu. Rev. Part. Nucl. Sci. **44**, 65 (1994), and references therein.
[5] R. Butsch, D. J. Hofman, C. P. Montoya, P. Paul, and M. Thoennessen, Phys. Rev. C **44**, 1515 (1991).
[6] D. J. Hofman, B. B. Back, I. Diószegi, C. P. Montoya, S. Schadmand, R. Varma, and P. Paul, Phys. Rev. Lett. **72**, 470 (1994).
[7] D. J. Hofman, B. B. Back, C. P. Montoya, S. Schadmand, R. Varma, and P. Paul, Phys. Rev. C **47**, 1103 (1993).
[8] P. Glässel, R. Schmidt-Fabian, D. Schwalm, D. Habs, and H. V. Helmdt, Nucl. Phys. **A502**, 315c (1989).
[9] F. S. Dietrich, J. C. Browne, W. J. O'Connell, and M. J. Kay, Phys. Rev. C **10**, 795 (1974).
[10] J. Kasagi, H. Hama, K. Yoshida, and M. Sakurai, Nucl. Phys. Soc. Jpn. **58**, 620 (1989).
[11] S. J. Luke, C. A. Gossett, and R. Vanderbosch, Phys. Rev. C **44**, 1548 (1991).
[12] H. van der Ploeg, R. Postma, J. C. S. Bacelar, T. van der Berg, V. E. Iacob, J. R. Jongman, and A. van der Woude, Phys. Rev. Lett. **68**, 3145 (1992); **69**, 1148(E) (1992).
[13] H. van der Ploeg, C. R. Laurens, J. C. S. Bacelar, A. Buda, J. J. Gaardhøje, G. van 't Hof, N. Kalantar-Nayestanaki, A. van der Woude, and Z. Zelazny, Nucl. Phys. **A569**, 83c (1994).
[14] H. van der Ploeg, Ph.D. thesis, University of Groningen, 1995.
[15] C. Budtz-Jørgensen and H. H. Knitter, Nucl. Phys. **A490**, 307 (1988).
[16] F. Pühlhofer, Nucl. Phys. **A280**, 267 (1977); M. N. Harakeh (extended version, private communication).
[17] K. A. Snover, Annu. Rev. Nucl. Part. Sci. **36**, 545 (1986).
[18] J. J. Gaardøje, Annu. Rev. Nucl. Part. Sci. **42**, 483 (1992).
[19] A. Bracco, J. J. Gaardhøje, A. M. Bruce, J. D. Garrett, B. Herskind, M. Pignanelli, D. Barneoud, M. Maurel, H. Nifenecker, J. A. Pinston, C. Ristori, F. Schussler, J. C. S. Bacelar, and H. Hofmann, Phys. Rev. Lett. **62**, 2080 (1989).
[20] D. R. Chakrabarty, S. Sen, M. Thoennessen, N. Alamanos, P. Paul, R. Schicker, J. Stachel, and J. J. Gaardhøje, Phys. Rev. C **36**, 1886 (1987).
[21] S. S. Dietrich and B. L. Berman, At. Data Nucl. Data Tables **38**, 199 (1988).
[22] S. Raman, C. H. Malarkey, W. T. Milner, C. W. Nestor, and P. H. Stelson, At. Data Nucl. Data Tables **36**, 1 (1987).
[23] Y. Alhassid and B. Bush, Nucl. Phys. **A509**, 461 (1990).
[24] J. P. S. van Schagen, Y. Alhassid, J. C. S. Bacelar, B. Bush, M. N. Harakeh, W. H. A. Hesselink, H. J. Hofmann, N. Kalantar-Nayestanaki, R. F. Noor-man, A. J. M. Plompen, A. Stolk, Z. Sujkowski, and A. van der Woude, Phys. Lett. B **343**, 64 (1995).
[25] R. F. Noorman, J. C. S. Bacelar, M. N. Harakeh, W. H. A. Hesselink, H. J. Hofmann, N. Kalantar-Nayestanaki, J. P. S. van Schagen, A. Stolk, Z. Sujkowski, M. J. A. de Voigt, and A. van der Woude, Nucl. Phys. **A574**, 501 (1994).
[26] H. W. Schmitt, J. H. Neiler, and F. J. Walter, Phys. Rev. **141**, 1146 (1966).
[27] B. D. Wilkins, E. P. Steinberg, and R. R. Chasman, Phys. Rev. C **14**, 1832 (1976).
[28] R. W. Hasse, Ann. Phys. (N.Y.) **68**, 377 (1971) (see Table A.III.b).
[29] K. Skarsvåg, Phys. Rev. C **22**, 638 (1980).
[30] W. Dilg, W. Schantl, H. Vonach, and M. Uhl, Nucl. Phys. **A217**, 269 (1973).
[31] H. J. Hofmann, J. C. Bacelar, M. N. Harakeh, T. D. Poelhekken, and A. van der Woude, Nucl. Phys. **A571**, 301 (1994); H. J. Hofmann, Ph.D. thesis, University of Groningen, 1991, Chap. 3.
[32] J. J. Gaardhøje, A. Atac, A. Maj, A. Bracco, F. Camera, B. Million, M. Pignanelli, and E. Rebesco, Nucl. Phys. **A538**, 573c (1992); A. Maj, J. J. Gaardhøje, A. Atac, S. Mitarai, J. Nyberg, A. Virtanen, A. Bracco, F. Camera, B. Million, and M. Pignanelli, *ibid.* **A571**, 185 (1994).